INSTITUTE FOR INFORMATICS AND AUTOMATION PROBLEMS OF THE NAS RA

Hayk Gasparyan

ENHANCING SOLAR PANEL ANALYTICS THROUGH RGB-MULTISPECTRAL DECOMPOSITION AND HARMONIC NETWORKS

ABSTRACT

of the dissertation for obtaining a Ph.D. degree in Technical Sciences on specialty 05.13.05 “Mathematical modelling, numerical methods and program complexes”

Yerevan 2025

ՀՀ ԳԱԱ ԻՆՖՈՐՄԱՏԻԿԱՅԻ ԵՎ ԱՎՏՈՄԱՏԱՑՄԱՆ ՊՐՈԲԼԵՄՆԵՐԻ ԻՆՍՏԻՏՈՒՏ

Հայկ Առնակի Գասպարյան

Արևային Պանելների Վերլուծության Բարելավումը Օգտագործելով RGB-ից Մուլտիսպեկտրալ Տրոհում և Հարմոնիկ Ցանցեր

Ե.13.05 - «Մաթեմատիկական մոդելավորում, թվային մեթոդներ և ծրագրերի համալիրներ» մասնագիտությամբ տեխնիկական գիտությունների թեկնածուի գիտական աստիճանի համար

ՍԵՂՄԱԳԻՐ

Երևան 2025

Relevance of the Research

Solar Photovoltaic (PV) energy is now among the leading renewable energy sources worldwide. The global installed capacity for solar PV increased from roughly 40 Gigawatt (gW) in 2010 [1] to more than 1.6 Terawatt (tW) by 2023 [2], driven primarily by the decreasing cost of solar modules, favorable clean energy policies, and growing investments from both the government and private sectors. Despite this growth, the profitability of large-scale solar farms remains sensitive to different factors. The performance of PV modules largely depends significantly on environmental conditions (e.g., dust, snow, shading), internal module faults (e.g., poor connections), and outer physical conditions (such as cracks, hot spots), as demonstrated in Figure 1. Field data and financial analyses indicate that these faults lead to three significant impacts:

- **Tiny hidden faults** like dust that shades a cell, hair-line cracks, bad connectors, or hot-spots trim about **3–5% of yearly output**. Field inspections show that **1–12%** of modules already have such defects within the first two years, and unchecked hot-spots may even ignite fires [3], [4].

- Only a **1%** annual decrease in solar plant performance can translate into **€3** billion lifetime revenue losses, significantly affecting the financial viability of large-scale installations [5]. Current studies estimate global annual losses due to undetected faults between **€3** and **€15** billion.

- Well-kept modules typically fade by only **0.5%** per year, staying close to **90%** of their power after **20 years** [6]. Dirt, moisture, and thermally stressed hot-spots speed annual degradation beyond **1%**, cutting useful life and forcing earlier, costly replacements [7].

Therefore, monitoring and maintaining optimal solar panel performance is crucial to minimizing energy production losses.

Currently, three primary approaches exist for monitoring PV installations, each with unique costs, accuracy, and operational constraints (as described in Table 1).

Manual inspection methods involve visual checks, thermal imaging, and electroluminescence testing. Although these methods can provide detailed assessments, they are expensive, costing approximately $1,500$ per Megawatt (mW), and are highly labor-intensive, requiring over 25 hours per $1,000$ panels. Current global installations translate into roughly 45 continuous years of inspection work. Additionally, the accuracy of manual inspections is limited, with error rates reaching up to 30%, mainly due to human factors [8], [9]. This translates into $\approx 6\%$ annual energy loss.

Alternatively, **embedded sensor** systems offer automated continuous monitoring by embedding sensors and Internet of Things (IoT)-based devices directly into PV arrays. Despite their automation advantages, these systems have substantial initial costs, reaching approximately $10,000 per MW. Additionally, embedded sensors typically require replacement every 2-5 years due to performance degradation, significantly increasing operational costs. Measurement inaccuracies from these sensors can reach more than 2%, potentially leading to significant annual production losses of around 7-10% [10].

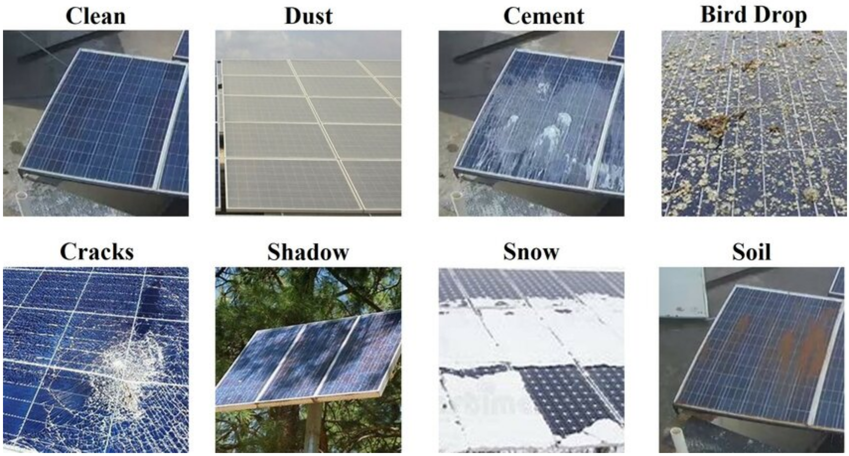

Figure 1: Solar PV fault examples.

Table 1: Comparison of PV-array monitoring approaches

Metric	Human Inspection	Embedded Sensors	UAV Monitoring
Typical cost	$\leq$ \$1,500 MW^{-1}	$\approx$ \$10,000 MW^{-1}	50-90% cheaper
Inspection time	$\leq 25\,\mathrm{h\,MW}^{-1}$	Real-time, continuous	$\sim 85\%$ faster
Maintenance cycle	Crew on demand	Swapped every 2-5 yr	Battery recharge
Accuracy/error	Up to 30% error	$\gtrsim 2\%$ sensor error	1-5% false detections
Energy impact	$\approx 5-6\%$ annual loss	$\approx 7-10\%$ annual loss	$\approx 0.5\%$ residual loss

In contrast, **UAV-based** monitoring provides a promising alternative that addresses many limitations of the previous methods. UAV monitoring substantially reduces operational expenses by 50-90%, compared to manual inspections and embedded sensor systems. [11]. Furthermore, UAV inspections can save approximately 85% time to cover equivalent areas [12], and through advanced deep learning analytics, UAV systems achieve fault detection accuracies between 95% and 99%, which translates into an estimated annual losses of just about 0.5% [13].

Camera Types. The first vital factor is the choice of camera. Different cameras significantly impact efficiency, performance, accuracy, and cost. In this field, four primary camera categories are used, each possessing distinct strengths and limitations. Table 2 summarizes the advantages and disadvantages of these camera types.

1. **Visible Red-Green-Blue (RGB) camera** captures three discrete spectral bands corresponding to red, green, and blue light. These images typically offer high spatial resolution but limited spectral detail. RGB cameras are also sensitive to noise and varying lighting conditions. However, their widespread availability and relatively low cost make them a common choice.

TABLE 2: Comparison of camera types for solar panel monitoring

Camera Type	Bands	Advantages	Disadvantages
Visible RGB	3 (Red, Green, Blue)	High spatial resolution; widely available; low cost.	Limited spectral detail; sensitive to noise and lighting variations.
Thermal	1 (Infrared)	Effective at detecting temperature differences and hot spots.	Lower spatial resolution; high-end units are relatively expensive.
Electroluminescence (EL)	1 (Emitted under electrical bias)	Reveals micro-cracks, inactive cells, and contact defects.	Requires dark conditions and external power; bulky and expensive equipment.
Multispectral	4-400+ narrow bands	Rich spectral information; Non-sensitive to environmental effects.	Heavy and costly; less practical for UAV deployment.

2. **Thermal camera** records emitted infrared radiation in a single spectral band, making it effective for detecting temperature variations on solar panels. Despite their effectiveness, thermal images typically possess lower spatial resolution and might miss fine structural details. Additionally, high-quality thermal cameras are significantly more expensive than standard RGB cameras.

3. **Electroluminescence (EL) camera** generates single-band images capturing electroluminescent emissions from electrically biased panels. EL imaging effectively identifies micro-cracks, inactive cells, and contact defects. However, EL cameras require dark conditions and an external power source to energize panels. Thus, EL cameras cannot operate independently on UAV platforms and typically serve as supplementary devices. Additionally, their relatively large size and higher cost further constrain their UAV applicability.

4. **Multispectral camera** captures numerous narrow spectral bands (up to hundreds in the case of hyperspectral cameras), providing detailed spectral information, which is crucial for precise material discrimination. While multispectral imaging is highly effective for monitoring tasks due to its comprehensive spectral detail, these cameras are heavier and considerably more expensive, limiting their suitability for UAV applications.

Multispectral Cameras. Multispectral cameras record a scene with N narrow wavelength bands, rather than a standard sensor's three broad RGB channels. The raw data form a spectral cube

$$I(x, y, \lambda_k), \qquad k = 1, \ldots, N,$$

where each band index k captures a small wavelength window

$$\left[\lambda_k - \tfrac{\Delta\lambda}{2},\, \lambda_k + \tfrac{\Delta\lambda}{2}\right],$$

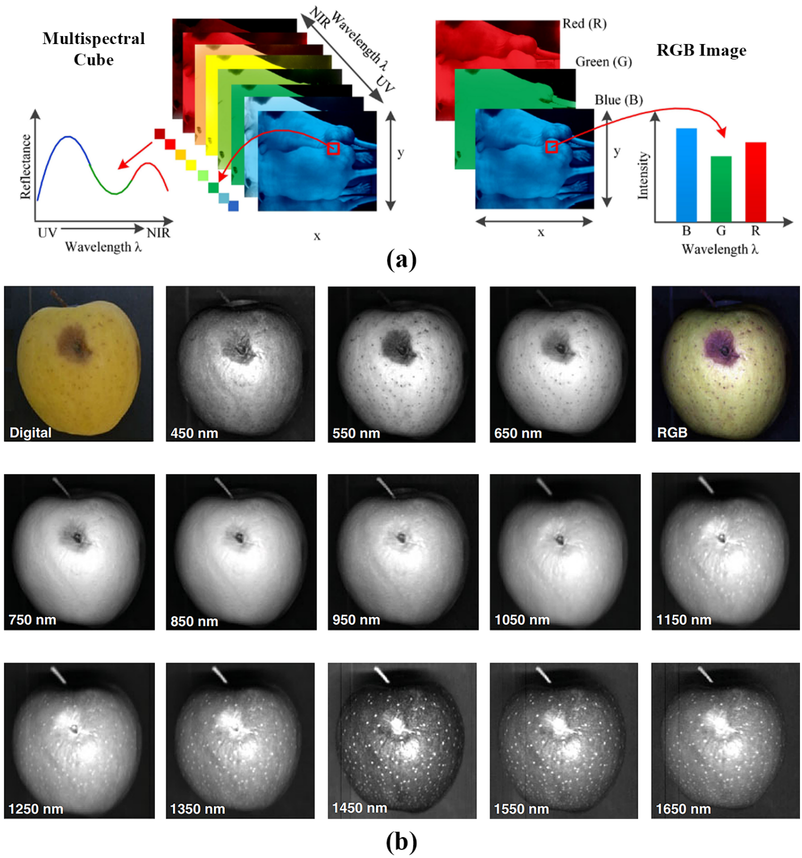

FIGURE 2: (a) Comparison of Multispectral and RGB images with their corresponding wavelengths [14], **(b)** example of multispectral image. Each band corresponds to a specific wavelength, representing different types of features [15]

centered at λ_k (for example, $\lambda_1 = 450\,\text{nm}$, $\lambda_2 = 550\,\text{nm}$, and so on). Each pixel is therefore described by an N-dimensional spectral vector

$$\mathbf{r}(x, y) = \big[I(x, y, \lambda_1),\, I(x, y, \lambda_2), \ldots, I(x, y, \lambda_N)\big]^\top,$$

Figure 2 (a) shows the difference between this concept and a standard RGB image. On the left, the stack of colored slices represents the N individual bands that make up a multispectral cube; the curve represents the intensities of wavelengths λ_k in a small patch or pixel. On the right, an RGB camera compresses the same scene into only three wide channels, shown by the blue, green and red bars; spectral information is averaged across bands into three channels.

Figure 2 (b) demonstrates the practical benefit: the healthy skin of an apple is bright in the near-infra-red (NIR) band at $\lambda = 750\,\text{nm}$, while a hidden bruise absorbs NIR and appears dark in that slice. In the short-wave range ($1350\,\text{nm}$ to $1650\,\text{nm}$) additional small surface defects become visible. Once the bands are separated, these faults are easy to detect.

The same principle works for solar panel inspection. Silicon cells (solar panels are made of silicon) show characteristic absorption in the short-wave range ($1100\,\text{nm}$ to $1500\,\text{nm}$), so panels can be better visible in just two or three specific λ_k bands while remaining almost invisible in raw RGB. Algorithms that work on $\mathbf{r}(x, y)$ instead of (R, G, B) reach 10-20 % higher F_1 scores for segmentation and fault classification [16]. Despite all these advantages, multispectral cameras can bring additional complexity and challenges.

Challenges of multispectral cameras

1. **Non real-time operations:** The majority of multispectral systems depend on *spatial scanning* [17]. The reason is that the sensor must traverse the scene or wavelength range sequentially.

2. **Motion:** Multispectral cameras have more prolonged exposure or scan times, which make it difficult to capture scenes that contain **motion**. Some solutions, such as mosaic filter arrays [18] bring a speed close to real-time multispectral capture. Still, they decrease the spectral and spatial resolutions, which are the main advantages of multispectral cameras.

3. **Cost:** Even low-cost multispectral/hyperspectral cameras remain expensive (typically \$ 10-\$100k), heavy, and power-consuming, limiting their usage on UAV platforms. These factors limit the widespread deployment of multispectral/hyperspectral cameras in drone-based applications.

4. **Band size:** The band size of multispectral images can have up to 400 channels (called a hyperspectral camera), and their processing requires a lot of computational power. Moreover, much of the information can be unnecessary and acts as noise for algorithms.

Challenges in UAV-based monitoring pipeline

- **Input image quality:** Input RGB images captured in aerial images often suffer from low visibility, low quality, noise, poor contrast, and other degradations, making subsequent algorithms less accurate.

- **Solar panel localization:** Solar panels must be automatically detected or segmented in the image. Such algorithms help to analyze only solar panel regions, ignoring complex background scenes.

- **Fault classification:** Faults must be classified into different types.

- **Accuracy and computations:** All these challenges must be solved with high precision and accuracy, while maintaining minimal computational complexity.

To overcome these challenges and limitations, this thesis introduces a Multispectral Decomposition (MD) method that generates multispectral bands from a standard RGB image. MD "decomposes" RGB data into separate spectral channels, offering multispectral-like features with affordable, lightweight RGB cameras. We demonstrate that MD significantly improves performance on critical monitoring tasks, addressing real-world challenges in solar panel inspection.

The Goal of the Thesis

The goal of this thesis is to address the challenges presented above and develop reliable, fast, and accurate deep learning based Computer Vision (CV) algorithms/models essential for an advanced automated solar PV monitoring system. To achieve this goal, the following technical tasks are set:

1. Develop a general RGB-to-multispectral decomposition network
2. Design an efficient spectral band selection strategy
3. Develop an efficient Chebyshev transformation-based segmentation framework
4. Implement an efficient and accurate harmonic **fault classification** networks
5. Evaluate the system on key metrics, including accuracy, computational complexity, and generalization to other applications

Structure of the Thesis

Figure 3 illustrates the structure of the thesis, its Chapters, their connections, and corresponding contributions in the overall system.

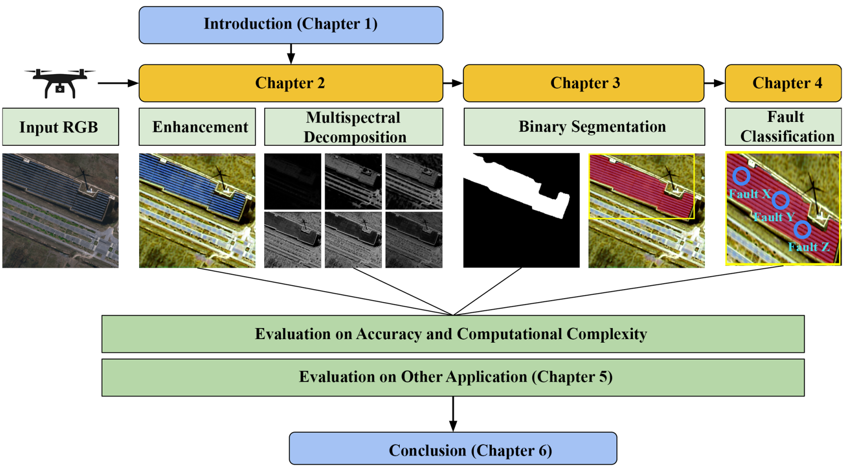

Figure 3: Structure of the thesis.

Chapter 1 serves as an introduction. It gives the definition and the motivation of the problem, highlights main challenges, sets the goal of the thesis and technical objectives, provides main contributions, lists the publications in the scope of this thesis, and emphasizes the impact of the thesis.

Chapter 2 aims to develop a generalized multispectral decomposition framework that addresses critical limitations of existing RGB-to-spectral reconstruction methods. Despite achieving very low pixel-wise reconstruction errors, current deep learning-based approaches still suffer from poor generalization across diverse lighting conditions and varying camera sensors. Besides, they cannot decompose a variable number of spectral bands, resulting in redundant, blurred, and less informative outputs. Moreover, they lose crucial details and lack evaluation on downstream remote sensing tasks. To overcome these challenges, this Chapter proposes **Retinex-based** [19] spectral reconstruction pipeline. First, an illumination-invariant enhancement step is introduced, ensuring consistent performance across diverse real-world scenarios. The step is designed to extract intrinsic *reflectance* R and scene *illumination* L from UAV imagery. Here R contains the materials' colors and fine textures of the scene and is invariant to lighting, whereas L is a smooth, single-channel map that captures overall brightness. According to Retinex theory [19], an observed RGB image I can be expressed pixel-wise as

$$I(x, y) = L(x, y)\, R(x, y), \qquad (x, y) \in \Omega. \tag{1}$$

The problem is that both L and R are unknown, and it makes this extraction an *ill-posed* problem: infinitely many pairs (L, R) satisfy the same product. To find an optimal solution, this Chapter introduces an RSD-Net [35], a two-branch network trained on matched *low-* and *normal-illumination* views of the same scene. Next, a developed Frequency Enhanced Multi Stage Transformer (FEMST) network decomposes *256* spectral bands. Over-

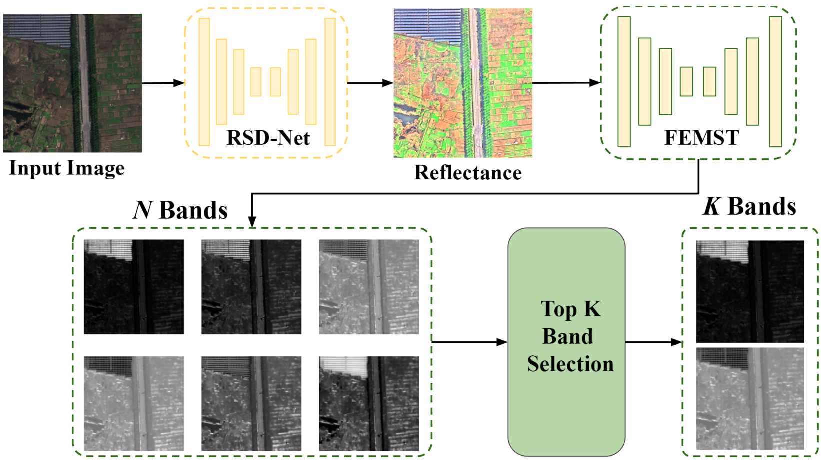

Figure 4: Overall pipeline of Multispectral Decomposition (MD) framework

Table 3: NTIRE 2022 HSI validation results.

Method	Params (M)	FLOPs (G)	MRAE↓	RMSE↓	PSNR↑	ES↑
HSCNN+ [20]	4.65	304.45	0.3814	0.0588	26.36	0.802
HRNet [21]	31.70	163.81	0.3476	0.0550	26.89	0.812
EDSR [22]	2.42	158.32	0.3277	0.0437	28.29	0.845
AWAN [23]	4.04	270.61	0.2500	0.0367	31.22	0.861
HDNet [24]	2.66	173.81	0.2048	0.0317	32.13	0.870
HINet [25]	5.21	31.04	0.2032	0.0303	32.51	0.882
MIRNet [26]	3.75	42.95	0.1890	0.0274	33.29	0.886
Restormer [27]	15.11	93.77	0.1833	0.0274	33.40	0.887
MPRNet [28]	3.62	101.59	0.1817	0.0270	33.50	0.890
MST-L [29]	2.45	32.07	0.1772	0.0256	33.90	0.894
MST++ [30]	**1.62**	23.05	0.1645	0.0248	34.32	0.903
FEMST (Ours)	1.72	**19.9**	**0.1405**	**0.0197**	**35.12**	**0.912**

Table 4: Retinex decomposition results on LOL dataset.

Model	PSNR	SSIM	RMSE	MRAE
R2RNet [31]	20.21	0.816	0.115	0.105
Retinex-2021 [32]	16.77	0.562	0.248	0.129
Deep Retinex [33]	16.77	0.425	0.275	0.272
KinD++ [34]	21.80	0.829	0.102	0.098
RSD-Net (Ours)	**22.49**	**0.845**	**0.085**	**0.083**

all pipeline of the framework is presented in Figure 4. FEMST uses a novel frequency-based attention block, which reduces spectral redundancy and enhances distinctiveness among neighboring bands. Finally, a band selection is designed to select the top K bands (user determines K depending on the task).

The main results in this chapter are the improved quality of reflectance extraction and the better general decomposition of multispectral bands from RGB images. Strong computer simulations prove the superiority of RSD-Net and FEMST against other state-of-the-art methods. Key image similarity and reconstruction metrics (such as PSNR, SSIM, RMSE) are utilized for evaluation. Additionally, this chapter proposes an entropy-based **(ES)** measure for quantifying spectral information in bands, which is a gap in existing methods. Two benchmark datasets (**LOL** [33] and **ARAD-1k** [36]) are used for the training and comparison of the proposed 2 networks with existing state-of-the-art methods. Tables 3 and 4 summarize the results and show that the proposed networks outperform existing methods across different metrics.

Chapter 3 creates a Solar Panel Segmentation (SPS) framework, called MSS-Net (Multispectral Segmentation Network) [37], which is **first** to utilize Multispectral Decomposition (MD) for the segmentation task. The MD (from Chapter 2) solves challenges that

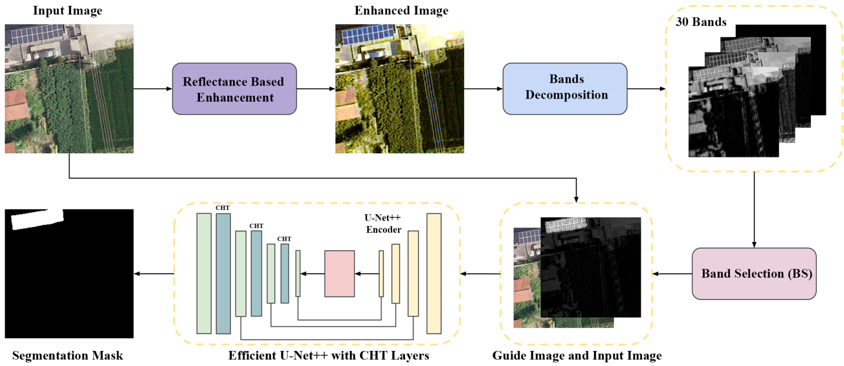

FIGURE 5: Overall architecture of MSS-Net

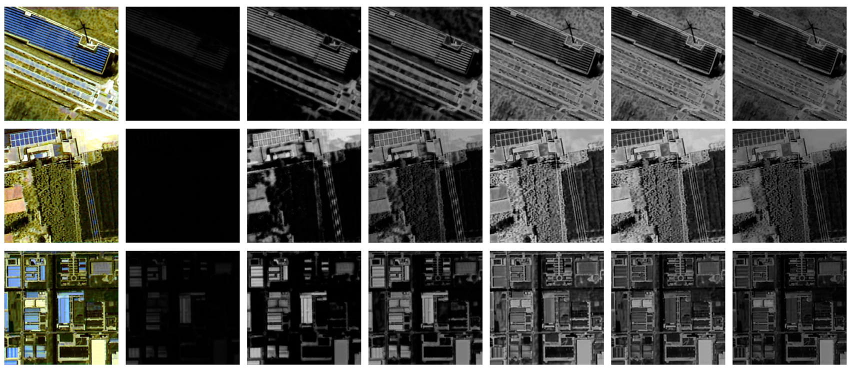

FIGURE 6: Band decomposition results for some band indexes: **a)** reflectance image **b)** index 1 **c)** index 5, **d)** index 10 **e)** index 15, **f)** index 25, **g)** index 30.

most segmentation methods face during remote sensing image analytics. They often fail to adequately consider the intrinsic physical characteristics of solar panels, such as color and texture, which often translates into false positive errors. Besides that, remote sensing aerial images commonly have low resolution and various degradations, which pose a challenge in differentiating small panels from their surroundings. Moreover, their high computational demands and large trainable parameter size limit real-time applications and their generalization to different complex scenes. To address these challenges, this Chapter integrates a multispectral decomposition framework, introduced in Chapter 2. An efficient band selection mechanism is designed to select the optimal bands, containing rich information about solar panels, and reduce the information from other objects. This minimizes the possible false positive errors of other SOTA methods. Moreover, a Chebyshev Transformation (CHT) layers are introduced and integrated in the network to keep it efficient and reduce trainable parameters, thus reducing overfitting and generalization errors. Figure 5 illustrates the architecture of MSS-Net, and Figure 6 shows some of the decomposed bands. The presented method is validated on three publicly available SPS benchmark datasets (BDAPPV [38], PV [39], and DeepSolar [40]). The comparison of the performance of MSS-Net is made against other methods, including CNN-based and transformer-based networks, showing that the proposed framework outperformed all SOTA methods across several key evaluation metrics, while reducing the trainable parameter size multiple times. Moreover, the ablation study analysis shows the effectiveness of each module, including the multispectral decomposition step.

Chapter 4 solves the main fault classification task in the monitoring pipeline. Existing Visual Transformer (ViT)s are considered as SOTA models in classification tasks, but have limitations such as quadratic computational complexity and a large training dataset requirement. As demonstrated in this Chapter, some redundancy of learned features also arises from self-attention blocks. To address these limitations, this Chapter aims to develop lightweight and efficient Fast Fourier Trasnform Power Coefficient (FFT-PC) and Slant Fast Orthogonal Transformation (SFOT) modules to replace existing self-attention layers of visual transformers, achieving comparable accuracy to vision transformers while significantly enhancing computational efficiency. In parallel, the Spatial Power Coefficient (S-PC) module uses architectural concepts from [41] to enhance edges in the spatial domain, fusing its output with FFT-PC in the frequency domain.

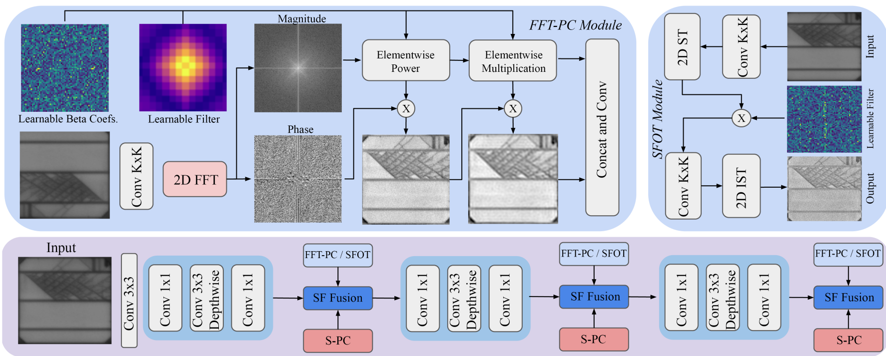

Figure 7: Overall architecture of MobileFFT or MobileSFOT.

Two new networks are developed based on FFT and Slant transformations, called *MobileFFT* and *MobileSFOT*, which are illustrated in Figure 7. Compared to standard transformer-based attention blocks, the proposed approach achieves approximately $4\times$ fewer Giga Floating-Point Operation (GFLOP)s (1.26 GFLOPs), $\sim 2.5\times$ fewer parameters (1.45 M), reduced inference latency, reduced Graphics Processing Unit (GPU) memory usage, and lower energy consumption (as shown in Table 5). This allows near-real-time Central Processing Unit (CPU) performance with low classification error and high precision (Figure 8).

Chapter 5 evaluates the generalization and performance of the multispectral decomposition-based pipeline on other tasks. This Chapter proposes a novel solution (*MSSOD-Net*) [42] to solve Salient Object Detection (SOD) problem. SOD aims to identify the most visu-

TABLE 5: Comparison of computational complexities

Model	**Params.**	**GFLOPS**	**Thrp. GPU**	**Thrp. CPU**	**Energy**	**Power**
MobileNetV3	1.50	<u>0.15</u>	<u>98</u>	<u>875</u>	<u>5.17</u>	<u>99.2</u>
EfficientNet	7.70	1.75	48	393	24.30	109.5
DenseNet121	7.00	7.46	37.6	292	31.90	124.5
DaViT-T	27.50	12.94	52.1	419	49.10	133.5
GCViT-xxt	11.48	3.90	49	300	30.50	112.0
MobileViT-xs	2.00	1.86	59	420	14.80	121.7
DFFformer-s18	28.00	9.93	24	164	66.40	112.8
GFNet	7.10	10.00	54	345	34.70	121.4
MobileFFT	<u>1.45</u>	1.59	97	558	9.80	105.4
MobileSFOT	<u>1.45</u>	1.26	71	506	8.40	102.7
MobileFFT-light	**0.70**	**0.14**	**194**	**915**	**3.40**	**91.5**
MobileSFOT-light	**0.70**	**0.11**	**168**	**850**	**3.20**	**89.9**

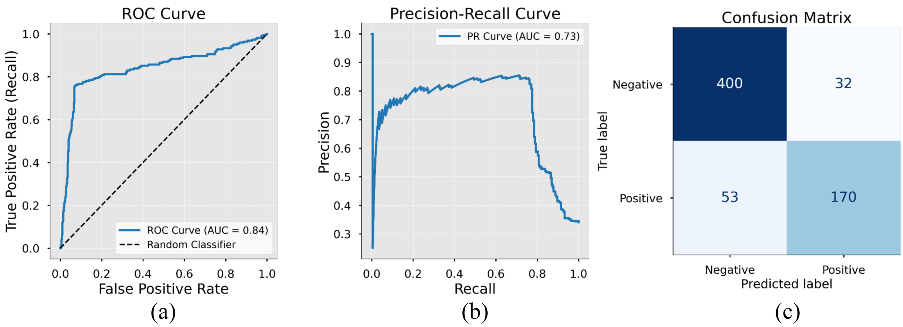

FIGURE 8: Results of MobileFFT network on ELPV binary classification dataset. **(a)** ROC curve, **(b)** Precision-Recall curve, and **(c)** confusion matrix.

ally prominent objects in images, crucial for tasks like image segmentation, visual tracking, autonomous navigation, and photo cropping. Initially, the RGB image is enhanced and decomposed into multiple spectral bands, enhancing the representation of salient features by capturing richer spectral information. Next, the bands containing the most salient information are identified and selected using a newly developed **entropy-based measure** operating in the frequency domain. A new synthetic RGB image is generated through the chosen bands, emphasizing salient objects more distinctly than the original input. Finally, a segmentation model processes the fused input (original and synthetic RGB), significantly improving the accuracy and reliability of salient object segmentation, especially in complex remote sensing scenarios. Figure 9 illustrates the overall architecture of the pipeline. Comprehensive experiments on publicly available benchmark datasets validate the superior performance of MSSOD-Net compared to state-of-the-art approaches. Table 6 shows the successful detection of salient objects by MSSOD-Net across several metrics compared to other state-of-the-art methods. The experiments demonstrate that the proposed multi-

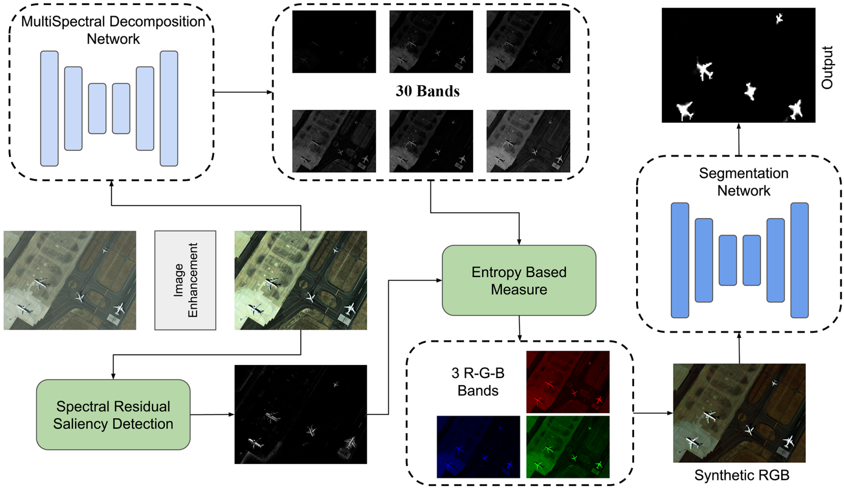

FIGURE 9: Overall architecture and workflow of MSSOD-Net.

TABLE 6: Quantitative comparison of proposed method against others on EORSSD dataset

	S-Measure↑	MAE↓	adpFM↑	meanFM↑	maxFM↑	adpEM↑	meanEM↑	maxEM↑
SRS	0.485	0.178	0.647	0.524	0.612	0.323	0.192	0.253
GCR	0.568	0.158	0.484	0.577	0.670	0.204	0.330	0.403
DeepLabV3	0.826	0.018	0.826	0.874	0.902	0.602	0.682	0.711
GSANet	0.801	0.025	0.834	0.856	0.871	0.616	0.670	0.689
MSSOD-Net	**0.841**	**0.017**	**0.854**	**0.881**	**0.912**	**0.637**	**0.703**	**0.731**

spectral decomposition method effectively generalizes to a broader range of remote sensing applications beyond solar panel monitoring tasks.

Chapter 6 concludes the thesis and summarizes the results and key contributions.

Contributions and Impact

The key contributions of the proposed methods and frameworks are:

1. Introducing FEMST, a novel multispectral decomposition framework featuring RSD-Net and frequency-attention blocks.

2. Developing MSS-Net, the first multispectral segmentation pipeline utilizing Chebyshev transformations.

3. Proposing lightweight transformer modules based on harmonic transforms instead of self-attention layers, significantly reducing computational complexity, energy consumption, and redundant information in transformers.

4. Evaluating the Multispectral Decomposition (MD) pipeline by extending it to salient object detection (SOD), achieving superior performance via a new entropy-based band selection metric.
5. Extensive benchmarking demonstrating the superiority of developed frameworks against existing state-of-the-art models

List of Author's Publications

1. [35] **(Q1, IF - 3.4)** - Gasparyan, H. A., Hovhannisyan, S. A., Babayan, S. V., Agaian, S. S. (2023). Iterative Retinex-based decomposition framework for low-light visibility restoration. IEEE Access, 11, 40298-40313. **(Chapter 2)**
2. [37] **(Q1, IF - 7.5)** - Gasparyan, H. A., Davtyan, T. A., Agaian, S. S. (2024). A novel framework for solar panel segmentation from remote sensing images: Utilizing Chebyshev transformer and hyperspectral decomposition. IEEE Transactions on Geoscience and Remote Sensing. **(Chapter 3)**
3. [43] **(Q1, IF - 5.6)** - Gasparyan, H., Agaian, S., Wu, S. (2025). Efficient Lightweight Networks for Solar Panel Fault Classification Using EL and RGB Imagery. IEEE Transactions on Instrumentation and Measurement. **(Chapter 4)**
4. [42] - Gasparyan, H. A. (2024). A Multispectral Decomposition and Frequency-Based Framework for Salient Object Detection in Remote Sensing Images. Mathematical Problems of Computer Science, 62, 93-111. **(Chapter 5)**

Impact - This thesis makes a strong contribution to industry and academia by presenting a general framework that extracts multispectral-level insight from an RGB camera. Besides the main problems this thesis addresses, it can impact other domains as well:

1. **Bridges, pipelines, and power-line corridors** and other structures can be surveyed in a single pass with a low-cost camera.
2. **In agriculture**, UAVs can map water deficits, dry areas, yield variations, plant diseases, and animals. The system can easily detect and segment every category of interest using multispectral bands.
3. **Military** applications have tasks that rely on night-vision, infrared, or near-infra-red (NIR) imagery. The proposed methodology can enhance low-light scenes and extract infrared-like bands from the multispectral decomposition.
4. **In computer vision research**, a paired RGB-multispectral dataset can be generated for training and benchmarking.
5. **Biotech and healthcare** can benefit from the proposed framework by getting spectral channels from standard microscopes. This can be combined with automatic segmentation in tissue and cell studies.

Bibliography

[1] I. Pvps, “Trends in photovoltaic applications. survey report of selected iea countries between 1992 and 2011,” *Report IEA-PVPS T1*, vol. 21, 2012.

[2] A. Jäger-Waldau, “Snapshot of photovoltaics- february 2024,” *EPJ photovoltaics*, vol. 15, p. 21, 2024.

[3] C. Deline, M. Muller, R. White, *et al.*, “Availability and performance loss factors for us pv fleet systems,” National Renewable Energy Laboratory (NREL), Golden, CO (United States), Tech. Rep., 2024.

[4] C. Schill, A. Anderson, C. Baldus-Jeursen, *et al.*, “Soiling losses–impact on the performance of photovoltaic power plants,” *International Energy Agency*, 2022.

[5] A. Trinks, M. Mulder, and B. Scholtens, “External carbon costs and internal carbon pricing,” *Renewable and Sustainable Energy Reviews*, vol. 168, p. 112 780, 2022.

[6] D. C. Jordan and S. R. Kurtz, “Photovoltaic degradation rates—an analytical review,” *Progress in photovoltaics: Research and Applications*, vol. 21, no. 1, pp. 12–29, 2013.

[7] S. A. A. Dos Santos, J. P. N. Torres, C. A. Fernandes, and R. A. M. Lameirinhas, “The impact of aging of solar cells on the performance of photovoltaic panels,” *Energy Conversion and Management: X*, vol. 10, p. 100 082, 2021.

[8] S. S. Akay, O. Özcan, O. Özcan, and Ö. Yetemen, “Efficiency analysis of solar farms by uav-based thermal monitoring,” *Engineering Science and Technology, an International Journal*, vol. 53, p. 101 688, 2024.

[9] M. Le, D. Le, and H. H. T. Vu, “Thermal inspection of photovoltaic modules with deep convolutional neural networks on edge devices in auv,” *Measurement*, vol. 218, p. 113 135, 2023.

[10] A. Baklouti, L. Mifdal, S. Dellagi, and A. Chelbi, “An optimal preventive maintenance policy for a solar photovoltaic system,” *Sustainability*, vol. 12, no. 10, p. 4266, 2020.

[11] Z. B. Duranay, “Fault detection in solar energy systems: A deep learning approach,” *Electronics*, vol. 12, no. 21, p. 4397, 2023.

[12] U. Pruthviraj, Y. Kashyap, E. Baxevanaki, and P. Kosmopoulos, “Solar photovoltaic hotspot inspection using unmanned aerial vehicle thermal images at a solar field in south india,” *Remote Sensing*, vol. 15, no. 7, p. 1914, 2023.

[13] A. Michail, A. Livera, G. Tziolis, *et al.*, “A comprehensive review of unmanned aerial vehicle-based approaches to support photovoltaic plant diagnosis,” *Heliyon*, vol. 10, no. 1, 2024.

[14] D. Cubero Valentín, “Machine learning for analysis of hyperspectral images,” B.S. thesis, Universitat Politècnica de Catalunya, 2022.

[15] M. S. Kim, S. R. Delwiche, K. Chao, *et al.*, “Visible to swir hyperspectral imaging for produce safety and quality evaluation,” *Sensing and Instrumentation for Food Quality and Safety*, vol. 5, pp. 155–164, 2011.

[16] R. Duan and Z. Ma, "A method for detecting photovoltaic panel faults using a drone equipped with a multispectral camera," *ISPRS Annals of the Photogrammetry, Remote Sensing and Spatial Information Sciences*, vol. 10, pp. 59–65, 2024.

[17] J. J. Sousa, P. Toscano, A. Matese, *et al.*, "Uav-based hyperspectral monitoring using push-broom and snapshot sensors: A multisite assessment for precision viticulture applications," *Sensors*, vol. 22, no. 17, p. 6574, 2022.

[18] B. Geelen, N. Tack, and A. Lambrechts, "A compact snapshot multispectral imager with a monolithically integrated per-pixel filter mosaic," in *Advanced fabrication technologies for micro/nano optics and photonics VII*, SPIE, vol. 8974, 2014, pp. 80–87.

[19] E. Land and J. L. MCCANN, "Retinex theory," *Journal of the Optical Society of America*, vol. 61, no. 1, pp. 1–11, 1971.

[20] Z. Xiong, Y. Shen, and J. Smith, "Hscnn+: A hybrid cnn for hyperspectral reconstruction from rgb," in *ECCV Workshops*, 2020.

[21] J. Wang, K. Sun, T. Liu, B. Shi, D. Huang, and Y. Tan, "Deep high-resolution representation learning for visual recognition," in *IEEE/CVF Conference on Computer Vision and Pattern Recognition (CVPR)*, 2020.

[22] B. Lim, S. Son, H. Kim, S. Nah, and K. Mu Lee, "Enhanced deep residual networks for single image super-resolution," in *IEEE Conference on Computer Vision and Pattern Recognition Workshops (CVPRW)*, 2017.

[23] H. Zhang and V. M. Patel, "All-in-one image restoration with flexible attention module," in *IEEE/CVF Conference on Computer Vision and Pattern Recognition (CVPR)*, 2021.

[24] X. Guo, X. Du, Y. Zou, and J. Wang, "Hdnet: A high-definition network for image restoration," in *European Conference on Computer Vision (ECCV)*, 2022.

[25] W. Chen and I. V. Bajic, "Hinet: Hierarchical image denoising network," in *European Conference on Computer Vision (ECCV)*, 2022.

[26] S. W. Zamir, A. Arora, S. Khan, M.-H. Yang, and L. Shao, "Mirnet: Multi-path residual interaction network for image restoration," in *IEEE/CVF Conference on Computer Vision and Pattern Recognition (CVPR)*, 2021.

[27] S. W. Zamir, A. Arora, S. Khan, Y. Kim, M.-H. Yang, and L. Shao, "Restormer: Efficient transformer for high-resolution image restoration," in *IEEE/CVF Conference on Computer Vision and Pattern Recognition (CVPR)*, 2022.

[28] S. W. Zamir, A. Arora, S. Khan, M.-H. Yang, and L. Shao, "Multi-path residual network for fast image restoration," in *European Conference on Computer Vision (ECCV)*, 2022.

[29] X. Liu, Y. Zhao, J. Chen, X. Li, S. Wang, and S. Kim, "Mst-l: A lightweight multiscale transformer for spectral reconstruction," in *IEEE International Conference on Image Processing (ICIP)*, 2023.

[30] Y. Cai, J. Lin, Z. Lin, *et al.*, "Mst++: Multi-stage spectral-wise transformer for efficient spectral reconstruction," in *Proceedings of the IEEE/CVF Conference on Computer Vision and Pattern Recognition*, 2022, pp. 745–755.

[31] J. Hai, Z. Xuan, R. Yang, *et al.*, "R2rnet: Low-light image enhancement via real-low to real-normal network," *Journal of Visual Communication and Image Representation*, vol. 90, p. 103 712, 2023.

[32] Z. Jiang, H. Li, L. Liu, A. Men, and H. Wang, "A switched view of retinex: Deep self-regularized low-light image enhancement," *Neurocomputing*, vol. 454, pp. 361–372, 2021.

[33] C. Wei, W. Wang, W. Yang, and J. Liu, "Deep retinex decomposition for low-light enhancement," *arXiv preprint arXiv:1808.04560*, 2018.

[34] Y. Zhang, X. Guo, J. Ma, W. Liu, and J. Zhang, "Beyond brightening low-light images," *International Journal of Computer Vision*, vol. 129, pp. 1013–1037, 2021.

[35] H. A. Gasparyan, S. A. Hovhannisyan, S. V. Babayan, and S. S. Agaian, "Iterative retinex-based decomposition framework for low light visibility restoration," *IEEE Access*, vol. 11, pp. 40 298–40 313, 2023.

[36] B. Arad, R. Timofte, R. Yahel, *et al.*, "Ntire 2022 spectral recovery challenge and data set," in *Proceedings of the IEEE/CVF Conference on Computer Vision and Pattern Recognition*, 2022, pp. 863–881.

[37] H. A. Gasparyan, T. A. Davtyan, and S. S. Agaian, "A novel framework for solar panel segmentation from remote sensing images: Utilizing chebyshev transformer and hyperspectral decomposition," *IEEE Transactions on Geoscience and Remote Sensing*, vol. 62, pp. 1–11, 2024.

[38] G. Kasmi, Y.-M. Saint-Drenan, D. Trebosc, *et al.*, "A crowdsourced dataset of aerial images with annotated solar photovoltaic arrays and installation metadata," *Scientific Data*, vol. 10, no. 1, p. 59, 2023.

[39] H. Jiang, L. Yao, N. Lu, *et al.*, "Multi-resolution dataset for photovoltaic panel segmentation from satellite and aerial imagery," *Earth System Science Data Discussions*, vol. 2021, pp. 1–17, 2021.

[40] J. Yu, Z. Wang, A. Majumdar, and R. Rajagopal, "Deepsolar: A machine learning framework to efficiently construct a solar deployment database in the united states," *Joule*, vol. 2, no. 12, pp. 2605–2617, 2018.

[41] S. A. Hovhannisyan, H. A. Gasparyan, S. S. Agaian, and A. Ghazaryan, "Aed-net: A single image dehazing," *IEEE access*, vol. 10, pp. 12 465–12 474, 2022.

[42] H. A. Gasparyan, "A multispectral decomposition and frequency-based framework for salient object detection in remote sensing images," *Mathematical Problems of Computer Science*, vol. 62, pp. 93–111, 2024.

[43] H. Gasparyan, S. Agaian, and S. Wu, "Efficient lightweight networks for solar panel fault classification using el and rgb imagery," *IEEE Transactions on Instrumentation and Measurement*, 2025.

Ամփոփում

Հայկ Առնակի Գասպարյան

Արևային Պանելների Վերլուծության Բարելավումը Օգտագործելով RGB-ից Մուլտիսպեկտրալ Տրոհում և Հարմոնիկ Ցանցեր

Աշխատանքը նվիրված է արևային պանելների ավտոմատացված մշտադիտարկմանը՝ օգտագործելով RGB պատկերների մուլտիսպեկտրալ տրոհում և հարմոնիկ ցանցեր: Այն ուղղված է անօդաչու թռչող սարքերով (ԱԹՍ) իրականացվող տեսահսկման գործընթացի արդյունավետության, ճշգրտության և կիրառելիության զգալի բարելավմանը

Աշխատանքի արդիականությունը պայմանավորված է այն փաստով, որ արևային պանելների շահագործման ընթացքում առաջացող բազմաթիվ խնդիրների (փոշի, ճեղքեր, միացման խափանումներ, ստվերներ) հայտնաբերումը և վերլուծությունը բարդ գործընթաց է, ինչը հանգեցնում է զգալի էներգետիկ կորուստների: Մինչ այժմ կիրառվող մեթոդները (մարդկային վերահսկում, ներկառուցված սենսորային համակարգեր, ԱԹՍ-ներ) ունեն բազմաթիվ թերություններ՝ բարձր գին, ցածր արագություն, մեծ սխալանք և այլն:

Աշխատանքի հիմնական նպատակն է մշակել արդյունավետ, արագ և հուսալի խորքային ուսուցման տեսողական ալգորիթմներ, որոնք ապահովում են արևային պանելների ավտոմատ մշտադիտարկման բարձր մակարդակ՝ հաղթահարելով գոյություն ունեցող մեթոդների սահմանափակումները:

Գիտական նորույթը և հիմնական լուծված խնդիրները հետևյալն են՝

1. Առաջարկվել է **FEMST** նոր տրանսֆորմեր-ցանց, որը կատարում է RGB պատկերից մուլտիսպեկտրալ գոտիների տրուհում: Էֆեկտիվ տրոհման համար RGB պատկերից տարանջատվում է (RSD-ցանցի շնորհիվ) լուսավորությունից անկախ արտացոլման կոմպոնենտ, որը ծառայում է որպես մուտքային պատկեր FEMST-ի համար: FEMST-ն պարունակում է նոր մշակված հաճախականային տիրույթում գործող «ուշադրության» մեխանիզմներ (attention mechanisms):
2. Մշակվել է **MSS-Net** մուլտիսպեկտրալ հատվածավորման (segmentation) ալգորիթմ՝ Չեբիշևի ձևափոխության և գոտիների ընտրության նոր մեխանիզմով, որը զգալիորեն նվազեցնում է կեղծ-դրական սխալանքը:
3. Առաջարկվել են **MobileFFT** և **MobileSFOT** հարմոնիկ ցանցեր՝ հաճախականության տիրույթում աշխատող նոր տեսողական բլոկներով՝ զգալիորեն կրճատելով հաշվարկային և ալգորիթմիկ բարդությունը, ինչպես նաև հզորության և էներգիայի ծախսերը՝ պահպանելով բարձր ճշգրտություն:

4. Ներդրվել է նոր **էնտրոպիայի** վրա հիմնված ընտրության ցուցիչ, որը թույլ է տալիս ավտոմատ կերպով ընտրել առավել տեղեկատվական գոտիներ՝ մուլտիսպեկտրալ տրոհման արդյունքներից:
5. Ամբողջ ալգորիթմական շղթան փորձարկվել է **SOD (Salient Object Detection)** խնդրում: Ցույց է տրվել առաջարկվող ալգորիթմների ընդհանրացման կարողությունը այլ նշանակություն ունեցող խնդիրներում:

Աշխատանքի կիրառական և գիտական նշանակությունը

- Առաջարկվող համակարգը թույլ է տալիս ԱԹՍ-ներով հայտնաբերել արևային պանելների դեֆեկտները, ինչը կարող է էականորեն կրճատել էներգետիկ կորուստները և սպասարկման ծախսերը:
- Մշակված մեթոդներն ընդհանրացվող են այլ ոլորտներում՝ շինարարության մշտադիտարկում (խողովակներ, կամուրջներ), գյուղատնտեսական վերլուծություն (ջրի դեֆիցիտ, բերքատվություն, հիվանդությունների հայտնաբերում), ռազմական և անվտանգային խնդիրներ (գիշերային տեսանելիության բարձրացում, ինֆրակարմիր ալիքների կիրառում), ինչպես նաև կենսաբժշկական վերլուծություն:
- Ստացված արդյունքները կարող են հիմք հանդիսանալ գիտական և կիրառական մի շարք ուղղություններում, ինչպիսիք են հարմոնիկ ցանցերի օգտագործումը կիրառական խնդիրներում, մուլտիսպեկտրալ տվյալների հավաքածուների ստեղծումը, մուլտիսպեկրալ տեսախցիկների լավացումը, ինչպես նաև նոր խորը նեյրոնային ցանցերի նախագծումը:

Տեխնիկական գիտությունների թեկնածուի գիտական աստիճանի ստացման համար ներկայացվող ատենախոսության հիմնական արդյունքներն ու ներդրումները ապահովում են արևային պանելների մշտադիտարկման ոլորտում նոր որակի ավտոմատացված վերլուծություն՝ գերազանցելով մինչ այժմ գոյություն ունեցող մեթոդները ինչպես ճշգրտությամբ, այնպես էլ արագությամբ և գործնական կիրառելիությամբ:

Заключение

Гаспарян Айк Арнакович

Улучшение анализа солнечных панелей с помощью многоспектральной декомпозиции RGB и гармонических сетей

Работа посвящена автоматизированному мониторингу солнечных панелей с использованием мультиспектральной декомпозиции RGB-изображений и гармонических сетей. Целью исследования является существенное повышение эффективности, точности и практической применимости видеомониторинга, осуществляемого с помощью беспилотных летательных аппаратов (БПЛА).

Актуальность работы обусловлена тем, что обнаружение и анализ многочисленных дефектов, возникающих в процессе использования солнечных панелей (таких как пыль, микротрещины, нарушения соединений, затенение), представляет собой сложную задачу, напрямую влияющую на эффективность их работы и приводящую к значительным потерям энергии. Существующие на сегодняшний день методы мониторинга (ручной осмотр, встроенные сенсорные системы и использование БПЛА) обладают рядом ограничений и недостатков: высокая стоимость, ограниченная скорость работы, низкая точность и другие недостатки.

Основная цель работы — разработка эффективных, высокоскоростных и надёжных визуальных алгоритмов глубокого обучения, обеспечивающих высокий уровень автоматизированного мониторинга солнечных панелей и способных преодолевать ограничения существующих подходов.

Научная новизна и основные решенные проблемы заключаются в следующем:

1. Предложена новая трансформерная сеть **FEMST**, предназначенная для извлечения мультиспектральных полос из RGB-изображения. Для эффективного разложения из RGB-изображения предварительно выделяется компонент отражения (с помощью сети RSD), независимый от освещения, который затем используется в качестве входного изображения для FEMST. Архитектура FEMST включает в себя недавно разработанные механизмы внимания (attention mechanism), работающие в частотной области
2. Разработан алгоритм мультиспектральной сегментации **MSS-Net**, основанный на преобразовании Чебышёва и новом механизме выбора спектральных полос, который существенно снижает количество ложноположительных ошибок.
3. Предложены гармонические сети **MobileFFT** и **MobileSFOT**, оснащённые новыми визуальными блоками, работающими в частотной областиm которые значительно сокращают вычислительную и алгоритмическую сложность, а

также энергопотребление и ресурсные затраты, при этом сохраняя высокую точность.

4. Введён новый показатель выбора на основе **энтропии**, который позволяет автоматически определять наиболее информативные спектральные полосы из результатов мультиспектрального разложения.
5. Вся алгоритмическая цепочка была протестирована на задаче **SOD (Salient Object Detection).** Продемонстрирована способность предложенных алгоритмов к обобщению и применению в задачах с иной постановкой.

Прикладное и научное значение работы

- Предлагаемая система обеспечивает обнаружение дефектов солнечных панелейс помощью беспилотных летательных аппаратов, что способствует существенному снижению энергетических потерь и затрат на обслуживание.
- Разработанные методы обладают высоким потенциалом обобщения и могут быть применены в различных областях: мониторинг объектов строительства (трубопроводы, мостовые конструкции), аграрный анализ (дефицит влаги, оценка урожайности, выявление заболеваний), решения в сфере обороны и безопасности (улучшение ночного видения, использование инфракрасного диапазона), а также в биомедицинских исследованиях.
- Полученные результаты могут стать основой для дальнейших исследований и разработок в ряде научных и прикладных направлений, включая применение гармонических сетей в практических задачах, формирование мультиспектральных наборов данных, совершенствование мультиспектральных камер, а также проектировани новых архитектур глубоких нейронных сетей.

Основные результаты и научный вклад диссертации, представленной на соискание учёной степени кандидата технических наук, обеспечивают качественно новый уровень автоматизированного анализа в области мониторинга солнечных панелей, превосходящий существующие методы по точности, скорости обработки и практической применимости.